IVYSPRING INTERNATIONAL PUBLISHER

International Journal of Medical Sciences

2026; 23(5): 1630-1644. doi: 10.7150/ijms.119908

Review

Beyond Angiography: Integrating Advanced Diagnostic Modalities in Coronary Stent Restenosis—a Systematic Review

Zihan Liu[1]; Mingduo Zhang, MD[2]; Min Zhang, MD[2]; Xiantao Song, MD[2]✉; Dongfeng Zhang, MD[2]✉

1. Capital Medical University, Beijing, China.
2. Beijing Anzhen Hospital, Capital Medical University, Beijing, China.

✉ Corresponding authors: song0929@mail.ccmu.edu.cn, dongfengdoctor@outlook.com

Received: 2025.06.19; Accepted: 2026.03.03; Published: 2026.03.25

Abstract

In-stent restenosis (ISR) continues to be a significant problem after percutaneous coronary intervention (PCI), negatively affecting patient care. This review offers a thorough examination of current ISR diagnostic methods - which combine anatomical and functional assessments with cutting-edge technologies - with holistic recommendations for ISR management, from optimized prevention during PCI to effective treatment.

Anatomically, coronary angiography (CAG) persists as the gold standard, while intravascular ultrasound (IVUS) and optical coherence tomography (OCT) enhance stent optimization and ISR detection through high-resolution imaging. Functionally, fractional flow reserve (FFR) and instantaneous wave-free ratio (iFR) quantify ischemic risk, whereas non-invasive techniques like Computed Tomography-derived Fractional Flow Reserve (CT-FFR) and quantitative flow ratio (QFR) are transforming clinical paradigms. Multimodal imaging fusion and artificial intelligence markedly improve diagnostic accuracy and efficiency. Biomarkers and genomics are valuable tools for assessing ISR risk. Future directions emphasize integrated anatomical-functional-molecular assessments and AI-driven personalized management to refine ISR care and patient prognosis.

Keywords: in-stent restenosis, fractional flow reserve, multimodal imaging integration

1. Background

CHD is the leading cause of death from cardiovascular issues globally. Percutaneous coronary intervention (PCI) has become a standard treatment for CHD thanks to recent advancements in coronary intervention technologies. As a pivotal technique within PCI, coronary stent implantation markedly improves patient prognosis and therapeutic implications. The issue of In-stent Restenosis (ISR) remains a persistent challenge in the field of medicine. Systematic synthesis of recent advances in ISR research and optimization of diagnostic strategies is therefore of substantial clinical importance for guiding evidence-based decision-making.

ISR occurs when the artery narrows again after the stent is implanted, often due to excessive new tissue growth. ISR is angiographically characterized by a lumen narrowing of at least 50% of the vessel diameter associated with evidence of functional significance (ischemic symptoms or abnormal fractional flow reserve) or a luminal narrowing of at least 70% in the absence of ischemic symptoms within 5 mm proximal or distal of the implanted stent [1].

Advances in understanding ISR pathogenesis have refined diagnostic methodologies, while simultaneously laying a theoretical foundation for the prevention of ISR. Although coronary angiography (CAG) remains the diagnostic gold standard, intravascular ultrasound (IVUS) and optical coherence tomography (OCT) are increasingly prioritized for their high-resolution visualization of

vessel wall pathology.

The clinical importance of ISR lies not only in the severity of anatomical stenosis, but also in the impact on myocardial ischemia. Functional evaluations critically assess the ischemic burden and prognostic implications of ISR lesions. Despite their clinical value, functional assessments face practical limitations in widespread adoption. Meanwhile, advances in biomarker research offer additional diagnostic insights.

Advances in medical imaging, artificial intelligence (AI), and deep learning are creating new, non-invasive ways to evaluate function. Computed tomography angiography-derived FFR (CT-FFR) facilitates rapid hemodynamic profiling of ISR lesions without invasive catheterization. AI-powered deep learning algorithms autonomously characterize ISR lesion morphology and synthesize clinical data to predict progression risks and hemodynamic impacts. Such multimodal, non-invasive diagnostic methods offer potential for streamlining procedures, lowering expenses, and enhancing accessibility, ultimately broadening patient benefits.

2. Anatomical Evaluation

2.1 Coronary Angiography (CAG)

CAG remains the gold standard for assessing coronary artery stenosis. However, its clinical application is constrained by its invasive nature, high cost, and procedure-related complications, including vascular endothelial injury and pseudoaneurysm formation.

Conventional CAG struggles to delineate complex lesion morphology due to the diverse nature of coronary disease, encompassing varying degrees of severity and spatial patterns [2]. Future advancements will combine computer-assisted guidance with AI-powered systems to improve image recognition and registration, leading to more adaptable and effective image fusion techniques.

2.2 Coronary Computed Tomography Angiography (CTA)

CTA is a non-invasive imaging modality that provides detailed visualization of vascular walls and plaque characteristics, enabling the assessment of ISR severity and spatial distribution, while partially serving as an alternative to conventional CAG. Although CTA provides distinct advantages for diagnosing ISR, its accuracy can be affected by several factors, including stent artifacts, contrast concentration, and scan parameters [3,4]. Therefore, a comprehensive diagnostic approach that integrates additional modalities is essential. The limited spatial resolution of CTA hinders its ability to accurately assess intra-arterial inflammation and makes comprehensive plaque characterization a lengthy process [5]. Consequently, rapid quantitative identification of high-risk plaques and precise stratification of plaque-related risks remain significant clinical challenges.

Advancements in AI and deep learning have accelerated the development of real-time CTA-X-ray image fusion technology, demonstrating the potential for automated and intelligent image processing. A process of three-dimensional reconstruction of CTA data is followed by registration and integration with intraprocedural X-ray images to generate synthesized visualizations [6]. In ISR interventions, this approach enhances visualization of in-stent structures and facilitates accurate assessment of stent expansion and neointimal distribution, potentially reducing procedural time, contrast load, and radiation exposure while improving intervention safety and efficacy. Furthermore, real-time visual navigation substantially improves anatomical precision and biomechanical compatibility during interventional procedures, methodically enhancing post-procedural safety outcomes [7].

Current image fusion techniques are often tied to specific company-made equipment and lack universality. Despite this, CTA-real-time X-ray image fusion technology has shown significant promise in interventional navigation by combining 3D vascular modeling with 2D fluoroscopic image spatial registration. However, due to the complexity of lesions, it still faces challenges in addressing position-related differences that affect accuracy and in enabling precise dynamic monitoring of disease progression [8].

2.3 Intravascular Ultrasound (IVUS)

IVUS utilizes distinct signal characteristics generated by ultrasound waves penetrating tissues to acquire internal coronary artery images via a miniature probe, enabling tissue composition analysis. As the gold standard for plaque assessment, IVUS demonstrates strong concordance with histopathological findings, differentiating arterial wall layers and identifying atherosclerotic plaque components [9].

Major adverse cardiovascular events (MACE) serve as the primary hard endpoint for evaluating clinical outcomes and the efficacy of therapeutic interventions in ISR. The IVUS-XPL study reported that patients meeting IVUS optimization criteria exhibited significantly lower rates of MACE within several years compared to non-optimized cases [10]. In ISR, IVUS enables precise measurement of minimal

stent area, quantification of neointimal hyperplasia volume, and detection of edge dissection—all of which inform the mechanism and optimal treatment of restenosis.

Despite its diagnostic utility, IVUS is constrained by several clinical limitations. First, it requires specialized operator expertise and entails high equipment and procedural costs, limiting widespread adoption. Second, IVUS exhibits relatively low spatial resolution—typically approximately 150 μm axially and 300 μm laterally—which restricts its ability to detect minute lesions, subtle plaque changes, and minor degrees of stent malapposition [11]. Consequently, IVUS cannot accurately characterize the fine structural details of coronary plaques. Procedurally, standardized protocols for IVUS-guided stent optimization remain inconsistent, contributing to operator-dependent variability in stent selection, inflation pressure, and apposition assessment, thereby limiting procedural reproducibility [12]. Furthermore, IVUS fails to adequately evaluate multifocal or diffuse coronary lesions, limiting its utility in diffuse ISR where multiple stenotic segments within a single stent require assessment and where determining the hemodynamically significant culprit segment is critical for targeted repeat intervention [13].

ISR is not a histologically homogeneous phenomenon; it encompasses both benign fibrotic neointimal hyperplasia and high-risk neoatherosclerosis characterized by lipid-rich necrotic cores, calcification, and thin-cap fibroatheroma — distinctions with important prognostic and therapeutic implications. Virtual histology intravascular ultrasound (VH-IVUS) utilizes a four-color coding system to classify distinct lesion types, demonstrating strong histopathological correlation in both native and stented coronary segments, is uniquely positioned to make this distinction *in vivo* [14]. By integrating radiofrequency ultrasound backscatter data with amplitude information, VH-IVUS identifies specific plaque components and provides direct visualization of vessel wall pathology as a catheter-based intracoronary imaging modality. It allows detailed characterization of plaque composition, burden, distribution, and remodeling patterns, thereby enhancing diagnostic accuracy for borderline lesions [15]. Consequently, VH-IVUS enhances the detection of vulnerable plaques, facilitates the prediction of MACE, and refines therapeutic decision-making. Furthermore, VH-IVUS serves as a critical diagnostic adjunct for minute lesions that elude characterization by conventional angiography and clinical risk predictors. The technique also enables evaluation of neointimal tissue components within ISR lesions and identifies morphological features predictive of ISR recurrence [16].

Integrated backscatter intravascular ultrasound (IB-IVUS), IVUS near-infrared spectroscopy (IVUS-NIRS), and IVUS with automated differential echogenicity (ADE) offer distinct advantages for vascular tissue characterization. Specifically, IB-IVUS quantifies tissue-specific backscatter signal properties, enabling reliable differentiation between fibrous tissue, lipid-rich plaques, and calcified lesions. This capability facilitates assessment of atherosclerotic plaque stability [17]. Conversely, IVUS-NIRS represents a hybrid modality combining ultrasound-based structural imaging with near-infrared spectroscopic analysis. This integration permits comprehensive lesion assessment: IVUS characterizes vascular wall anatomy, while NIRS identifies lipid-rich and vulnerable plaques through chemical composition analysis. The approach is particularly valuable for ISR diagnosis, as it simultaneously visualizes neointimal hyperplasia within stents and characterizes its compositional features.

Moreover, ADE employs an automated algorithm to analyze echogenicity variations across tissue types. This enhances both the accuracy and efficiency of IVUS in classifying vascular lesion components [18]. By reducing subjectivity inherent in manual interpretation, ADE improves IVUS reliability for detecting vulnerable plaques and informing optimal interventional strategies.

2.4 Optical Coherence Tomography (OCT)

A pivotal mechanism underlying ISR is suboptimal stent apposition. This condition induces hyperproliferation of vascular endothelial and smooth muscle cells, culminating in recurrent luminal stenosis. OCT directly visualizes stent-vessel wall interfaces, enabling precise identification of malapposition sites—including edge dissections, inter-strut tissue prolapse, and incomplete stent expansion [19]. OCT has emerged as the reference standard for morphological characterization of ISR, providing detailed visualization of in-stent tissue that is essential for uproviding detailed coronary artery visualization and guiding phenotype-matched repeat intervention. It facilitates precise outlines of coronary anatomy, quantitative assessment of stenosis severity, and real-time guidance during PCI [20]. Moreover, OCT effectively detects thrombogenic risk factors, including stent malapposition, under expansion, and nascent atherosclerosis, thereby informing targeted interventions to mitigate stent thrombosis [21]. Compared with conventional CTA, OCT demonstrates superior performance in defining ISR

morphology through enhanced visualization of neointimal hyperplasia characteristics, including thickness stratification, spatial distribution patterns, and tissue homogeneity, enabling refined classification and severity grading [22].

However, OCT exhibits several limitations in ISR assessment: its imaging depth is confined to the vascular intima and partial media, restricting comprehensive evaluation of deep vascular pathologies and providing inadequate data for complex deep-layer lesions. Similar to IVUS, OCT requires specialized equipment, trained operators, and complex workflows, resulting in elevated procedural costs. Imaging acquisition necessitates patient cooperation and contrast flushing for blood clearance, posing challenges in patients with renal insufficiency or contrast allergies. Furthermore, rigorous blood clearance during OCT procedures may induce transient ischemic symptoms such as chest pain or angina, increasing procedural risks and potentially complicating assessment in patients with severe ISR where even transient ischemia is poorly tolerated [23–25].

A summary of key clinical technologies pertaining to imaging evaluation can be found in Table 1.

3. Functional Evaluation

While imaging-based diagnostic methods effectively evaluate coronary artery stenosis severity and lesion morphology, they lack precision in assessing the hemodynamic relationship between vascular narrowing and myocardial ischemia. Hemodynamic functional evaluation techniques determine whether myocardial ischemia coexists within the vascular territory, thereby guiding clinical decisions regarding coronary artery disease intervention. A summary of key clinical technologies pertaining to multimodal functional evaluation can be found in Table 2.

Table 1. Comparative analysis of coronary imaging technologies in the Context of ISR

	CAG	CTA	OCT	IVUS	VH-IVUS	IB-IVUS	ADE	NIRS	PCCT
Principle	X-ray imaging	CT technology 3D images	Infrared light interference imaging	HF-US and radiofrequency RF spectrum analysis	Color coding	Backscatter	Automated Differential Echogenicity	Near-infrared light absorption	X-ray imaging
Resolution	Relatively low	400-600 microns [3,4]	10 - 20 microns [21]	100 - 150 microns [11]					Superior spatial resolution [26]
Penetration Depth	Capable of penetrating the entire vascular lumen		1 - 2 millimeters	4 - 8 millimeters [11]					Moderate
Imaging Speed	Fast	Moderate	Fast	Slow, affecting imaging efficiency				Fast	Ultra-fast
Advantages	Accurate	Non-invasive	High resolution	Comprehensive vascular assessment and remodeling Assess stent expansion and malapposition					Reduced overestimation of calcification volume
Characteristics	2D	3D	Allowing more precise differentiation of vascular wall layers	Accurate evaluation of stent apposition and external compression	Identifying vulnerable and lipid-rich plaques	Enhanced discrimination between lipid-laden atherosclerotic lesions and high-risk vulnerable plaques	Mitigates the subjective bias characteristic of manual analytical approaches	Quantitative profiling of molecular constituents in endothelial layers	Enhanced visualization of intravascular microstructures and lesions
Clinical Application	Preliminary assessment Guidance for interventional procedures	Initial vascular assessment Guidance for stent implantation	Detection of TCFA Risk stratification Visualization of thin-layer intimal hyperplasia Prediction of stent under-expansion	Complex lesions long-segment vascular imaging left main coronary artery lesions				Morphological assessment of in-stent neointimal proliferation, intimal dissection, and thrombogenic activity	Detailed imaging of local lesions Simultaneous multi-coronary artery imaging Comprehensive observation
Limitations	Unable to show vessel wall details	Lower accuracy than CAG	Shallow imaging depth Susceptible to blood interference Inability to perform prolonged measurements	Constrained resolution Depends on operator's experience Restricted detection sensitivity for microstructural pathological alterations					Existence of noise interference Technically demanding High maintenance costs

Table 2. Comparative analysis of coronary multimodal functional technologies in the Context of ISR

	FFR	CT-FFR	QFR	OFR	UFR	RFR
Principle	Measure the pressure ratio between the distal end of the lesion and the aorta	Based on CTA Computational fluid dynamics 3D model	Based on CAG Computational fluid dynamics 3D model	Based on OCT High-resolution intraluminal information	Based on IVUS Intraluminal information	Ratio of distal coronary pressure to aortic pressure
Accuracy	Gold standard with high diagnostic accuracy, over 80% [35]	In accordance with FFR	High diagnostic accuracy, over 90% [58] Good correlation and consistency with FFR	High diagnostic accuracy, over 90% [62] Good correlation and consistency with FFR	High diagnostic accuracy, over 90% [66] Good correlation and consistency with FFR	Good correlation and consistency with FFR [52,53]
Convenience	Require drug induction and pressure-guided wire	Non-invasive Rapid No additional equipment or consumables are required	Require pressure-guided wire	Require dedicated equipment and specialized software for calculation	Require dedicated equipment and specialized software for calculation	No need for vasodilators
Invasive	√	×	√	×	×	√
Drug induction	√	×	×	×	×	×
Application scope	Assessment of coronary artery stenosis lesions Identify hemodynamic significance of ISR	Assessment of coronary artery stenosis lesions and plaque status Mainly used for screening and initial evaluation	Formulate revascularization strategies Assessment of bifurcation and diffuse lesions	Auxiliary tool for coronary artery intervention Facilitate assessment of stenting outcomes	Assessment of severe calcified lesions Reduce target lesion revascularization Assist in formulating interventional treatment strategies and long-term prognosis for left main coronary bifurcation lesions	Identify potentially overlooked lesions
Limitations	Require maximum hyperemia induction, which some patients tolerate poorly	Different algorithms vary in accuracy and reliability	Relatively high cost easily affected by intravascular blood, increasing computational complexity and error Less accurate than OFR and UFR in complex lesions Need large-scale studies	Relatively high cost Easily influenced by intravascular blood Need large-scale studies	Relatively high cost Depending on the operator's experience Less sensitive to fully reflecting individual hemodynamic differences Need large-scale studies	Susceptible to the influence of abnormal circulatory function Need large-scale studies

3.1 Fractional Flow Reserve (FFR)

Fractional flow reserve (FFR), an invasive hemodynamic index, represents the ratio of maximum achievable myocardial blood flow distal to a coronary stenosis to the theoretical maximum flow in the same vessel under normal conditions. In 1993, Pijls et al. first reported the seminal work establishing FFR methodology [27]. Previous studies demonstrated that an FFR threshold ≤0.80 reliably identifies myocardial ischemia associated with stenosis. The measurement protocol employs a 0.014-inch pressure wire to record distal coronary pressure, while proximal pressure is obtained via the guiding catheter. Vasodilators (e.g., adenosine or adenosine triphosphate) are administered during measurement to induce maximal hyperemia [28].

FFR reflects the relationship between coronary stenosis and myocardial perfusion, serving as the gold standard for evaluating the functional impact of coronary lesions. This technique provides hemodynamic data unaffected by heart rate, blood pressure, or acute hemodynamic changes, thus compensating for the anatomical limitations of CAG. When compared to CAG, FFR-guided PCI in patients with borderline lesions demonstrates significant clinical benefits, including reduced contrast usage and stent deployment, alongside improved patient outcomes and enhanced procedural safety [29]. Decreased FFR values within ISR lesions correlate with elevated risks of MACE, establishing FFR as a critical prognostic indicator for refined risk stratification [30]. The FAME3 trial identified post-PCI FFR as a significant predictor of target vessel failure at both vessel and patient levels, with lower post-PCI FFR values associated with higher revascularization rates [31].

Despite its clinical utility, FFR faces three principal limitations that are particularly pronounced in the assessment of ISR. First, its invasive nature carries inherent procedural risks, crossing the lesion with a pressure wire carries additional risk of dislodging fragile neointimal tissue or thrombus [32]. Second, adenosine administration is contraindicated in certain populations; in ISR patients, who are frequently older and have multiple comorbidities, the prevalence of such contraindications is notably higher. Even in eligible populations, 12%-18% of patients exhibit adenosine resistance, necessitating dose escalation that increases gastrointestinal adverse effects, such as nausea and vomiting, without guaranteeing optimal measurement conditions [33]. Third, microvascular dysfunction systematically compromises FFR accuracy by impairing maximal

hyperemic response, leading to underestimation of ischemic severity. This is especially critical in ISR patients, many of whom have underlying diabetic or chronic inflammatory conditions associated with microvascular disease. A multicenter prospective study by Seitz et al. found that in patients with FFR values greater than 0.80, those with concomitant microcirculatory dysfunction had a significantly increased risk of MACE within two years [34]. This suggests that relying solely on FFR may overlook the risks associated with microcirculatory abnormalities, necessitating combined assessment with coronary flow reserve. For ISR patients with preserved FFR, unrecognized microvascular dysfunction may lead to a false sense of security and undertreatment. Consequently, the consistency between FFR and myocardial perfusion imaging is reduced. Lee et al.'s analysis of 313 patients with high FFR (>0.80) further demonstrated that low coronary flow reserve and high microvascular resistance index independently predict adverse outcomes, highlighting microvascular pathology's prognostic significance even when normal FFR values [35].

The integration of FFR with imaging modalities enhances diagnostic precision [36]. Future developments aim to establish hybrid protocols combining anatomical and functional data for comprehensive coronary evaluation.

3.2 Instantaneous Wave-Free Ratio (iFR)

Instantaneous wave-free ratio (iFR) measures the ratio of distal coronary to aortic pressure during the diastolic wave-free period. While normal coronary vessels maintain constant pressure gradients along their course, stenotic lesions induce pressure decay due to energy dissipation. iFR delivers intracoronary pressure measurements equivalent to pressure wire-acquired FFR, utilizing pressure wire measurements without requiring vasodilators. Notably, iFR measurement optimizes clinical workflows through reduced assessment duration while offering distinct advantages for adenosine-contraindicated patients, a demographic overrepresented among those presenting with ISR [37].

However, a significant research gap exists: these pivotal trials largely excluded or did not specifically analyze patients with ISR. Berry et al.'s multinational longitudinal study demonstrates weak iFR-FFR correlation ($r=0.32$, $p<0.05$), fundamentally challenging its clinical utility in stenosis management [38]. The iFR framework, rooted in wave intensity analysis (WIA), defines quiescent phases, postulates pharmacotherapy-free vasodilation during diastolic pressure convergence. Experimental validation reveals iFR's inherent limitations as a microcirculatory resistance index, violating Ohm's law principles and demonstrating restricted stability across vasomotor states. While offering procedural efficiencies, iFR's clinical adoption remains limited by inadequate RCT validation and persistent hemodynamic modeling constraints. Current evidence for iFR in the specific context of restenotic lesions remains limited to small observational series, and long-term outcomes beyond five years for iFR-guided ISR management are entirely lacking. Conducting extended follow-up research is therefore imperative to comprehensively evaluate long-term outcomes, address this gap, and provide more robust clinical evidence.

4. Multimodal Imaging Integration for Diagnosis

4.1 CT-Derived FFR (CT-FFR)

Computed tomography-derived fractional flow reserve (CT-FFR) non-invasively calculates fractional flow reserve by applying computational fluid dynamics (CFD) and machine learning algorithms to CTA datasets [39]. Approved for clinical use in multiple regions, CT-FFR serves as a critical adjunct for screening, diagnosis, and revascularization decision-making.

This technology addresses a critical unmet need in ISR management: the lack of a non-invasive, accurate method for routine surveillance. As a non-invasive technique integrating anatomical and functional evaluation, CT-FFR eliminates procedural risks associated with invasive FFR and adenosine contraindications, particularly benefiting high-risk populations. By incorporating CTA-derived plaque characteristics (calcification distribution, plaque burden) with hemodynamic data, it provides comprehensive insights for managing diffuse and tandem lesions [40]. In post-PCI follow-up assessments, CT-FFR has demonstrated efficacy in identifying ISR and distal flow limitations, exhibiting high diagnostic concordance with invasive FFR measurements [41]. Multicenter validation studies have validated diagnostic reliability, with CT-FFR exhibiting strong correlations with invasive FFR and demonstrating ischemia-specific specificity of 84% in non-calcified lesions [42–44]. CT-FFR offers the potential for earlier detection of hemodynamically significant restenosis, enabling timely intervention before progression to myocardial infarction.

Despite its promise, the translation of CT-FFR into routine ISR surveillance faces several population-specific barriers. Current challenges include stringent CTA quality requirements and physiological variability. Optimized computational models and accelerated processing enable expanded

applications, including emergency settings. Cost-effectiveness analyses indicate CT-FFR reduces unnecessary revascularizations [45]. The PRECISE randomized trial first confirmed that a risk-stratified strategy based on CTA with selective FFR-CT can significantly optimize the treatment pathway for patients at high risk of ISR, reduce inefficient angioplasty, and identify high-risk ischemic lesions requiring intervention [46].

Technical constraints persist, particularly in severely calcified lesions, vessel tortuosity, and stent artifact interference (>0.05 FFR deviation). Accuracy diminishes in small distal vessels. Future developments focus on refining CFD models through shear stress analysis and artifact suppression [47]. AI-enhanced algorithms improve computational efficiency, while calcium correction and microvascular resistance modeling promise accuracy improvements [48]. The development and external validation of ISR-dedicated prediction models incorporating serial CT-FFR metrics represent a critical unmet need.

Multifactorial predictive models integrating clinical data, imaging features, and biomarkers enable early detection of ISR. These models improve risk stratification accuracy through multimodal data synthesis. He et al. developed and validated a nomogram-based prediction model incorporating clinical variables including diabetes mellitus, lesion length, and stent diameter, achieving robust discrimination for ISR risk stratification [49]. Similarly, Deng et al. reported that systemic immune-inflammation index, when integrated with angiographic features, significantly enhanced predictive performance for ISR compared to clinical factors alone [50]. Multimodal data synthesis combining clinical, imaging, and biomarker information represents a promising direction for precision medicine in ISR management, enabling earlier identification of high-risk patients and more targeted therapeutic interventions.

4.2 Resting Full-Cycle Ratio (RFR)

The functional assessment of ISR by hyperemic pressure indices is frequently compromised by the high prevalence of adenosine contraindications, adenosine resistance, and microvascular dysfunction in this population. Resting Full-Cycle Ratio (RFR) is an emerging tool for the functional assessment of coronary arteries. It utilizes the ratio of distal coronary pressure (Pd) to aortic pressure (Pa) across the entire cardiac cycle, offers a theoretical solution to this clinical dilemma. Unlike traditional indices that focus solely on specific cardiac phases, RFR integrates hemodynamic information from both diastole and systole, providing comprehensive assessment of restenotic lesion severity without pharmacological stress [51]. RFR demonstrates high diagnostic accuracy and excellent correlation with FFR [52,53], establishing its clinical validity. Notably, RFR exhibits robust discriminatory capacity, particularly in identifying hemodynamically significant stenoses potentially overlooked by conventional methods [54]. However, despite its advantages over other resting indices, RFR remains susceptible to confounding factors. In cases of abnormal coronary microcirculation, the results may be subject to certain interferences [55].

4.3 Quantitative Flow Ratio (QFR)

Quantitative Flow Ratio (QFR), an angiography-derived FFR technology originating in China, calculates fractional flow reserve via three-dimensional vascular reconstruction and computational fluid dynamics analysis of coronary angiography images. For ISR surveillance, where repeated invasive functional assessment is often deferred due to procedural concerns, QFR offers a mechanism to integrate physiological evaluation into every follow-up angiogram without additional risk or cost. The 2024 European Guidelines for Chronic Coronary Syndrome (CCS) Management designate QFR as a Class I recommendation, recognizing its role as a novel standard for coronary functional evaluation [56]. This guideline endorsement, while based primarily on *de novo* lesion data, establishes a framework for extending QFR to ISR assessment—a logical next step given the shared technical principles.

QFR demonstrates enhanced predictive performance for FFR assessment relative to conventional FFR and iFR techniques. This innovation derives its distinct procedural merits from obviating both intracoronary pressure wire deployment and pharmacological hyperemia induction, minimizing procedural complexity and patient discomfort while preserving diagnostic precision [57]. The clinical application value of QFR requires further prospective validation, particularly regarding hard endpoints. Measurement reproducibility is influenced by angiographic quality, observer-dependent stenosis assessment, and reference FFR values [58]. For ISR, these technical constraints are amplified by stent-related artifacts and the complex morphology of restenotic lesions, underscoring the need for ISR-specific validation studies.

By addressing key limitations of existing techniques, QFR exhibits heightened diagnostic performance, positioning it as a promising future standard for evaluating coronary physiological function [59]. However, the FAVOR III Europe trial

indicates QFR fails to demonstrate clinical outcome equivalence when invasive FFR is available. Conversely, evidence suggests QFR outperforms visual stenosis assessment in settings where FFR is inaccessible [60]. As it is based on CAG, QFR is an invasive test with complex procedures and a longer duration. It also involves significant radiation and contrast agent use, which is contraindicated for some patients. Moreover, its accuracy is compromised when evaluating highly complex lesions. Whether QFR can be widely used in CAD phenotypes remains to be seen. Its broad clinical potential requires further study.

4.4 Optical Flow Ratio (OFR)

ISR is characterized by distinct morphological phenotypes—ranging from homogeneous neointimal hyperplasia to heterogeneous neoatherosclerosis with high-risk plaque features—that can be precisely delineated by OCT but lack direct correlation with hemodynamic significance [61]. Optical flow ratio (OFR), an OCT-based innovation, rapidly computes FFR by integrating multidimensional OCT data. This evolution enables simultaneous assessment of plaque morphology and coronary physiology. It overcomes angiography limitations in lumen boundary detection—particularly calcium artifacts and contrast filling heterogeneity—thereby advancing integrated morpho-functional diagnostics [62]. OFR's unique algorithmic architecture maintains diagnostic accuracy irrespective of stent implantation status, suggesting robustness to metallic artifact [63]. This technical characteristic holds particular promise for ISR assessment, offering the potential to derive FFR-equivalent metrics without pressure wire traversal through restenotic tissue—avoiding theoretical risks of neointimal disruption and reducing procedural complexity.

Despite its advantages, OFR's clinical implementation faces critical barriers. Similar to early QFR development, multicenter randomized controlled trial evidence remains absent. Validation in high-risk plaque phenotypes and complex anatomies requires further investigation [64]. Future research should establish causal relationships between OFR-guided revascularization and MACE reduction while exploring synergistic applications with intravascular ultrasound and determining whether serial OFR assessment can predict ISR progression or guide personalized surveillance intervals in stented patients.

4.5 Intravascular Ultrasound-Based Fractional Flow Reserve (UFR)

Intravascular Ultrasound-Based Fractional Flow Reserve (UFR) is a novel method integrating IVUS imaging to determine whether anatomical findings correspond to hemodynamically significant flow limitation. A retrospective single-center study by Yu et al. shows that due to its short analysis time, UFR analysis can immediately assess the physiological significance of coronary stenosis right after IVUS image acquisition without extra instruments [65]. In the ISR context, this capability holds theoretical promise: it would enable operators to determine, during the same procedure, not only why the stent has restenosed (via IVUS) but also whether the restenosis is flow-limiting and requires intervention (via UFR).

Sui et al. compared UFR based on intravascular ultrasound with QFR based on angiography in diagnosing LMCA stenosis and showed that UFR has a strong correlation and good consistency with FFR [66]. Current evidence highlights the value of UFR in minimizing over-treatment and facilitating prognosis stratification, particularly in diffuse lesions and calcified nodules. UFR accurately assesses stenosis significance, identifies specific segments requiring dilation in diffuse lesions, and evaluates the hemodynamic impact of calcified nodules to guide treatment strategies such as calcium modification. However, direct evidence for UFR in ISR remains entirely absent, as validation studies explicitly excluded patients with prior stents. Consequently, the diagnostic accuracy, optimal thresholds, and prognostic value of UFR in restenotic lesions are completely unknown.

4.6 CTA-OCT/IVUS Integration

ISR represents a distinct disease entity characterized by in-stent neointimal proliferation and neoatherosclerosis, whose comprehensive evaluation requires integration of non-invasive detection, invasive mechanistic diagnosis, and risk stratification—a paradigm that mirrors the broader trend toward multimodal plaque characterization. While CTA provides detailed anatomical information about complex lesions, it lacks direct functional assessment. Intravascular imaging modalities (OCT/IVUS) enable precise intraprocedural evaluation for stent optimization. Growing evidence suggests no single technique comprehensively evaluates coronary atherosclerosis. Multimodal integration synthesizes morphological and compositional data, advancing the understanding of acute coronary syndrome (ACS) pathophysiology and guiding targeted therapies [67].

Voros et al., based on differences in CT attenuation values, highlighted the association between the imaging characteristics of non-calcified

plaques and their potential histological composition, establishing a foundation for CTA as an effective non-invasive tool for plaque characterization [68]. Furthermore, CTA surpasses CAG by enabling three-dimensional plaque characterization and identification of high-risk features. This positions CTA as an effective gatekeeper for invasive imaging, streamlining workflow through targeted patient selection, which reduces unnecessary procedures and focuses valuable resources on suspicious and complex lesions.

CTA and intravascular imaging (IVUS/OCT) serve complementary roles: CTA delivers a macroscopic stent overview, whereas IVUS/OCT provides microscopic structural details. Athanasiou L et al. confirmed a strong correlation between the luminal, outer vessel wall, and volumetric parameters obtained from IVUS and CTA, thereby validating the reliability of CTA-based models for non-invasive vascular assessment [69]. Cao et al. demonstrated the excellent diagnostic performance of CTA in detecting coronary plaque and accurately identifying its type, underscoring its significant value for risk stratification [70].

4.7 IVUS-OCT Dual-Modality Catheter

Multimodal imaging techniques have shown significant clinical potential for ISR diagnosis, Their core strength lies in integrating complementary data from distinct modalities to overcome limitations inherent in single-technique approaches. IVUS excels at detecting mechanical abnormalities—stent underexpansion, fracture, edge dissection—while OCT provides unparalleled resolution for characterizing in-stent tissue—neointimal patterns, neoatherosclerosis, thrombus, and uncovered struts. Through technical complementarity and data synergy, multimodal imaging enhances diagnostic accuracy and treatment monitoring, particularly in complex lesion management [71].

However, the high cost of the dual-modality IVUS-OCT system, along with its technical complexity and operational difficulty, somewhat limits its widespread application, making it challenging to implement in regions with limited medical resources. While the two systems are functionally complementary, there is a conflict between resolution and penetration depth. OCT offers high resolution but is limited in imaging depth, whereas IVUS has strong penetration but relatively low resolution, which may affect the comprehensive evaluation of certain lesions [72]. Furthermore, signal interference and artifacts can impact image quality and diagnostic accuracy, and currently, there is a lack of unified diagnostic standards.

AI-powered analysis of dual-modality imaging holds particular promise. Advancements in AI and miniaturization technologies position multimodal imaging as a cornerstone for precision coronary intervention, heralding an era of intelligent personalized cardiovascular care [73].

5. Biomarker Analysis

There have been significant advances in the study of molecular mechanisms of ISR. Biomolecular markers attract considerable research interest due to their potential in risk stratification, early diagnosis, and prediction of therapeutic efficacy. It is crucial to search for innovative therapeutic targets based on the pathogenesis.

Future ISR diagnosis will pivot toward the convergence of bioengineering, data science, and clinical medicine. This integration will advance management beyond traditional imaging and empirical approaches, enabling multidimensional, dynamic, and personalized strategies.

5.1 Inflammation-Related Markers

As a classic marker of inflammation, C-reactive protein (CRP) has been proven to be related to ISR risk in numerous studies [74,75]. Elevated plasma levels not only reflect the systemic inflammatory state but also promote vascular smooth muscle cell proliferation and neo-intimal formation by activating the NF-κB pathway in endothelial cells, suggesting its potential as an indicator of atherosclerosis progression [76]. Additional inflammatory mediators similarly predict ISR occurrence. Redox processes exacerbate the inflammatory response through the generation of reactive oxygen species (ROS) and reactive nitrogen species (RNS), leading to vascular smooth muscle cell proliferation and migration, thereby promoting ISR development. Inflammation and oxidative stress interact, creating a vicious cycle that drives the pathological process of ISR [77]. The neutrophil-to-lymphocyte ratio (NLR) elevation independently predicts ISR risk across diverse vascular conditions [78], with inflammation and oxidative stress forming a self-perpetuating pathological cycle.

5.2 Endothelial Dysfunction-Related Markers

Non-invasive endothelial function testing identifies endothelial dysfunction as a predictor of late ISR progression, offering diagnostic and prognostic utility [79]. Integration of genetic data on intimal hyperplasia-associated variants facilitates risk stratification and personalized monitoring. Bioinformatics analyses have further identified endothelial dysfunction-related genes as potential

therapeutic targets and diagnostic biomarkers for atherosclerotic risk assessment, providing supplementary ISR diagnostic support [80].

5.3 Genomic and Transcriptomic Markers

High-throughput sequencing reveals genetic susceptibility to ISR, with genome-wide association studies (GWAS) identifying multiple associated loci [81]. High-throughput sequencing enables patient-specific genetic risk score (GRS) construction to predict ISR probability, offering genetic adjuncts for diagnosis [82]. Additionally, AI-driven multimodal models that integrate clinical data, imaging features, and GRS can significantly enhance the accuracy of ISR risk prediction [82].

5.4 Emerging Therapeutic Targets and Marker-Target Integration

Some drug target-related molecules also have the potential to be biomarkers. Future large-scale prospective cohort studies should validate marker efficacy while exploring epigenetic regulation and endothelial-immune cell interactions in ISR pathogenesis. This approach will advance precision medicine through individualized diagnostic and therapeutic strategies.

6. Emerging Technologies

6.1 Photon-Counting CT (PCCT)

Photon-counting CT (PCCT), an emerging CT technology based on energy-resolving, direct-conversion X-ray detectors, captures the energy information of individual X-ray photons via photon-counting detectors (PCDs), achieving unprecedented spatial resolution (150–200 μm) with pixel sizes of 0.1–0.2 mm [83]. With its ultra-high resolution, multi-energy imaging, and low radiation dose characteristics, PCCT offers a new perspective for ISR diagnosis and mechanism research. By analyzing X-ray photon energy spectra, it differentiates material compositions precisely [26]. Its spectral imaging capability classifies photons into distinct energy bins, enabling advanced reconstruction techniques such as virtual non-iodine (VNI) and virtual monoenergetic images (VMI) [84]. PCCT demonstrates superior ISR diagnostic performance by enhancing spatial and contrast resolution with reduced noise and artifacts. It significantly decreases radiation exposure and contrast volume during CTA, particularly improving stent lumen visualization in severe calcification [85]. Combined with CT-FFR, PCCT enhances functional ISR assessment while minimizing invasive procedures for high-risk patients.

Leveraging multi-energy parametric imaging, PCCT discriminates materials by atomic number [86]. Beyond quantifying plaque burden, it identifies neointimal fibrous and lipid components and enables AI-driven volumetric measurements, informing intervention strategies.

Despite its theoretical advantages for non-invasive ISR surveillance, PCCT faces several challenges that currently limit its evidence-based application in this population, corresponding to specific knowledge gap. Although metal artifacts are reduced, high-atomic-number stents may still impair peri-stent imaging [87]. Current PCCT-ISR studies are limited by small sample sizes, requiring large-scale prospective validation.

6.2 Deep Learning-Based Reconstruction (DLR): AiCE System

Non-invasive ISR surveillance by CT has been historically limited by three interconnected challenges: cumulative radiation exposure from repeated imaging, image noise compromising detection of subtle in-stent changes, and metallic stent artifacts obscuring lumen visualization. The integration of machine learning (ML) addresses these challenges simultaneously, enhancing standardization across the ISR imaging chain. Its high accuracy and efficiency are crucial for clinical practice. The system aids physicians in more accurately diagnosing and treating stable angina patients, reduces unnecessary invasive procedures, and improves patient acceptance and early diagnosis feasibility [88].

For ISR, where even small improvements in diagnostic confidence can prevent unnecessary repeat catheterizations, AI-enhanced imaging offers a pathway to safer, more efficient diagnosis. The AI-powered AiCE system utilizes convolutional neural networks (CNNs) trained on high-resolution medical images to restore diagnostic-quality images from low-dose or noisy data. Using deep convolutional neural networks (DCNNs), AiCE learns features from model-based iterative reconstruction (MBIR) images to enhance hybrid iterative reconstruction (HIR) outputs, achieving MBIR-equivalent quality with reduced computational demands [89].

This technology distinguishes true signals from noise without increasing radiation, preserving anatomical fidelity critical for longitudinal comparison of in-stent luminal dimensions and early detection of restenosis progression. Integrated into CT workflows, AiCE delivers rapid, high-definition imaging. Recent developments apply deep learning to mitigate metal artifacts, outperforming conventional methods in primary and secondary artifact

suppression [90].

AI model performance critically depends on training data diversity. Limited demographic or equipment representation in training datasets may compromise generalizability and artifact correction stability. High-quality, multi-source annotated datasets are essential for algorithm robustness [91]. Deep learning reconstruction represents a paradigm shift for CT, MR, and PET imaging. For ISR in particular, it provides the technological foundation for a future in which surveillance is personalized, radiation-minimized, and invasively confirmed only when AI-flagged abnormalities warrant catheterization.

Table 3. Summary of Major Large-Scale Trials and Key Evidence

Study	Study type	Results	Clinical Significance
IVUS-XPL (IVUS) [10]	Randomized Clinical Trial	MACE incidence: 2.9% (IVUS-guided) vs. 5.8% (angiography-guided), P=0.007 TLR: 2.5% (IVUS-guided) vs. 5.0% (angiography-guided); HR 0.51, P=0.02 Cardiac death and target lesion-related MI were comparable between groups. Post-dilation was performed more frequently (76% vs. 57%), resulting in a larger final minimum lumen diameter in the IVUS-guided group.	Demonstrates superiority of IVUS-guided over angiography-guided second generation DES implantation in long lesions Provides high-level evidence supporting IVUS use in complex coronary intervention. Suggests IVUS reduces TLR risk by optimizing stent expansion and luminal gain. Supports routine IVUS use in long lesions to improve clinical outcomes.
iOPEN (IVUS) [11]	Single-center, observational, retrospective cohort study	MACE: 18.0% (IVUS-guided) vs. 24.5% (angiography-guided), p=0.0014 TLR: 14.5% (IVUS-guided) vs. 19.2% (angiography-guided); p=0.021 More frequent post-dilation (18.6% vs. 14.1%) Larger stent diameter (3.04 mm vs. 2.94 mm) in IVUS group Shorter hospitalization (2.1 vs. 2.5 days) with IVUS, despite longer procedure time and contrast volume	Provides large-scale real-world evidence for IVUS use in ISR-PCI IVUS guidance significantly reduces 1-year MACE risk in ISR patients Supports routine IVUS in ISR to identify failure mechanisms & optimize strategy
PRESTIGE (OCT) [19]	Multicenter, prospective, observational registry	DES implantation: Significantly associated with neoatherosclerosis, p=0.02	First large-scale prospective registry linking DES implantation with accelerated neoatherosclerosis Supports OCT's clinical utility for identifying high-risk plaque features Highlights need for vigilant monitoring of neoatherosclerosis in patients with prior MI
PRECISE (CT-FFR) [46]	Multicenter, prospective, randomized controlled trial	Primary Endpoint (Efficiency + Safety): 4.2% (Precision) vs. 11.3% (Usual), HR 0.35 Procedural Efficiency: Lower catheterization rate without obstructive CAD (2.6% vs. 10.2%) Safety: No significant difference in death/nonfatal MI Medical Therapy Optimization: Higher 1-year use of lipid-lowering (50.0% vs. 41.8%) and antiplatelet (35.7% vs. 27.1%) drugs in Precision group Diagnostic Precision: Fewer total tests, higher initial test positivity (18.3% vs. 13.3%), and higher diagnostic yield of obstructive CAD at catheterization (80.0% vs. 39.5%)	First large RCT demonstrating that a precision strategy using quantitative risk stratification (PMRS) with CTA/selective FFR-CT improves efficiency and reduces unnecessary procedures. Provides RCT evidence for risk-based testing and offers an actionable protocol. Increases diagnostic yield of catheterization and optimizes medical therapy without compromising safety.
VALIDATE (iFR) [52]	Retrospective, multicenter, diagnostic study	High Concordance: RFR highly correlated with iFR, R^2=0.99 Equivalent Diagnostic Performance: Accuracy 97.4% vs. iFR Cycle Phase Independence: Minimum Pd/Pa occurred outside diastole in 12.2% of cycles (32.4% in RCA). Statistical Diagnostic Equivalence: Met predefined equivalence criteria, p=0.03	Represents a potentially superior tool for non-hyperemic physiologic assessment with clinical translation potential
FAVOR III (QFR) [60]	Multicenter, randomized, sham-controlled, blinded clinical trial	1-year MACE incidence: 5.8% (QFR-guided) vs. 8.8% (angiography-guided), P=0.0004 Lower rates of MI (3.4% vs 5.7%) and ischemia-driven revascularization (2.0% vs 3.1%). Procedural Impact: QFR altered initial treatment strategy in 23.3% of patients, leading to fewer stents, less contrast, and shorter procedure time. Revascularization Quality: Higher rate of functional complete revascularization (88.1% vs 82.2%).	First large-scale RCT demonstrating that wire-free, angiography-based physiology (QFR) improves clinical outcomes post-PCI Offers a convenient, adenosine- and wire-free alternative to increase adoption of physiological assessment. Improves outcomes while reducing resource use (stents, contrast, radiation), indicating health economic benefits. Advances the shift from anatomy-guided to function-guided intervention, supporting QFR as a new standard of care.

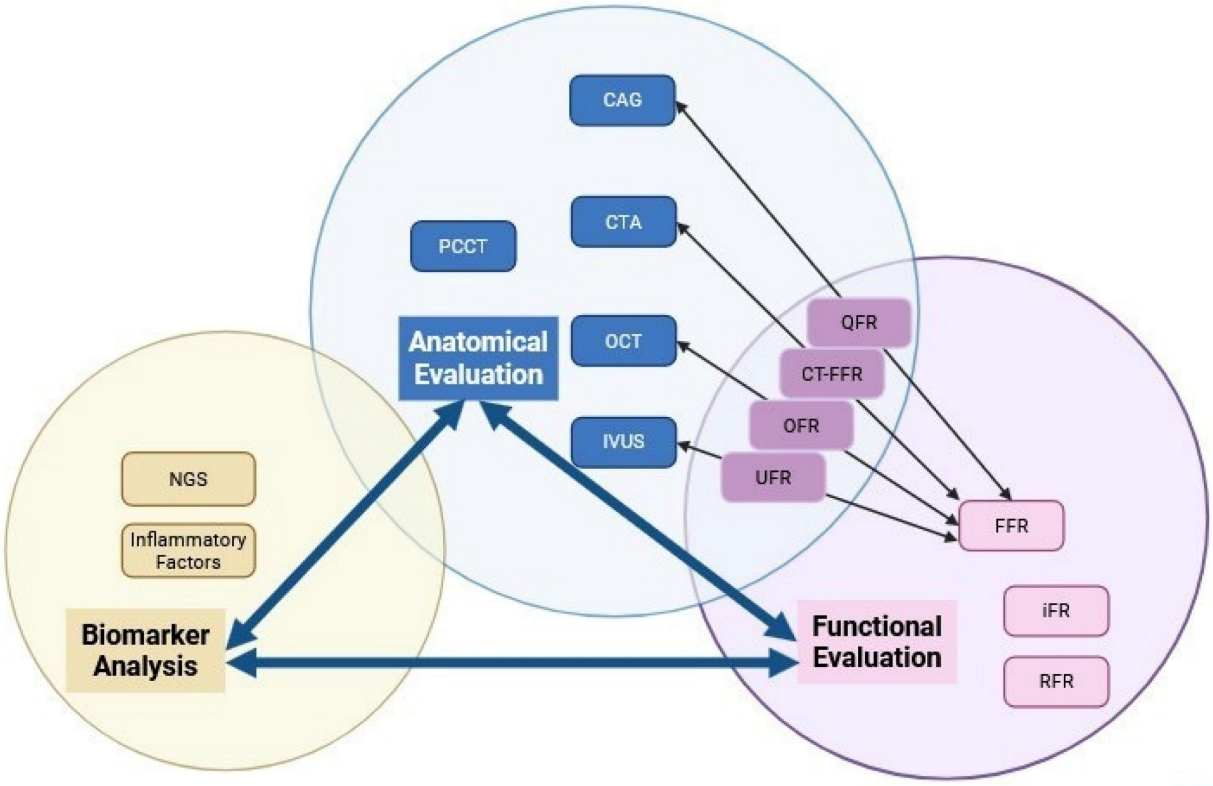

Figure 1 Categorization and Relationships Among Imaging Modalities. The diagram schematic illustrates the relationships of three primary evaluation domains: anatomical evaluation, functional evaluation, and biomarker analysis. It explicitly frames these as an interconnected diagnostic cascade, where each domain both informs and complements the others to enable comprehensive assessment.

7. Clinical Strategies and Discussion

ISR assessment requires combining anatomical, imaging, and functional data for a complete evaluation. CAG is the preferred initial diagnostic method due to its ease of access and quick results. Despite its capabilities, the method has limitations in identifying mild stenosis and struggles to accurately detect early signs of ISR. OCT and IVUS offer detailed vascular imaging with high-resolution images. These imaging techniques can identify neointimal hyperplasia and detect stent-related mechanical issues, providing crucial insights for treatment decisions.

Functional validation via methods like FFR and iFR is critical for moderate stenosis management. These assessments determine stenosis hemodynamic significance, guide treatment decisions, and ensure only functionally significant lesions are treated. For high-risk individuals, regular monitoring of inflammatory biomarkers and imaging helps to provide a more complete picture. This method enables early identification of ISR and facilitates adjustments to treatment plans to prevent serious complications. Multimodal imaging integration has revolutionized ISR diagnosis. CT-FFR, QFR, OFR, UFR, and RFR offer unique benefits. The combined approach provides a complete assessment of ISR, encompassing both anatomical and functional aspects. This multi-dimensional approach enhances early ISR detection, supports lesion-specific treatment, improves outcomes, and advances precision medicine in interventional cardiology.

The evolution of ISR diagnosis has shifted from traditional anatomical assessment to sophisticated multimodal functional evaluation. The shift towards improved ISR detection and subtype classification is fueled by advancements in technologies such as PCCT, AI, and novel biomarkers. AI integration with multimodal imaging analysis is becoming central to ISR diagnosis. AI algorithms can analyze vast data from different imaging modalities and clinical parameters, identifying patterns and correlations. Advanced technologies and AI-powered multimodal analysis create effective and accurate diagnostic tools. By utilizing these frameworks, clinicians can conduct thorough evaluations, leading to improved patient outcomes through early intervention and tailored treatment plans. A schematic conclusion ofthe relationships in between three primary evaluation domains can be found in Figure 1.

Abbreviations

ISR: In-stent Restenosis; PCI: Percutaneous Coronary Intervention; MACE: Major Adverse

Cardiovascular Events; CAG: Coronary Angiography; CTA: Coronary Computed Tomography Angiography; OCT: Optical Coherence Tomography; IVUS: Intravascular Ultrasound; VH-IVUS: Virtual Histology Intravascular Ultrasound; IB-IVUS: Integrated Backscatter Intravascular Ultrasound; ADE: Automated Differential Echogenicity; NIRS: Near-Infrared Spectroscopy; PCCT: Photon-Counting CT; TCFA: thin-cap fibroatheroma; FFR: Fractional Flow Reserve; CT-FFR: Computed Tomography-derived Fractional Flow Reserve; iFR: instantaneous wave-free ratio; QFR: Quantitative Flow Ratio; OFR: Optical Flow Ratio; UFR: Intravascular Ultrasound-Based Fractional Flow Reserve; RFR: Resting Full-Cycle Ratio; AI: Artificial Intelligence; RCT: Randomized Controlled Trial; LMCA: Left Main Coronary Artery; CRP: C-Reactive Protein; PCCT: Photon-Counting CT; NGS: Next-Generation Sequencing.

Acknowledgments

The authors thank Beijing Nova Program (Z211100002121056), and Beijing Hospital Authority Cultivation Program (PX20250602), for all artistic support related to this work.

Declaration of Generative AI and AI-assisted Technologies in the Writing Process

During the preparation of this work the authors used ChatGPT in order to improve language. After using this tool, the authors reviewed and edited the content as needed and take full responsibility for the content of the publication.

Competing Interests

The authors have declared that no competing interest exists.

References

1. Giustino G, Colombo A, Camaj A, Yasumura K, Mehran R, Stone GW, et al. Coronary In-Stent Restenosis. Journal of the American College of Cardiology. 2022 Jul;80(4):348–72. doi:10.1016/j.jacc.2022.05.017
2. Khan SU, Agarwal S, Arshad HB, Akbar UA, Mamas MA, Arora S, et al. Intravascular imaging guided versus coronary angiography guided percutaneous coronary intervention: systematic review and meta-analysis. BMJ. 2023 Nov 16;383:e077848. doi:10.1136/bmj-2023-077848 PubMed PMID: 37973170; PubMed Central PMCID: PMC10652093.
3. de Graaf FR, Schuijf JD, van Velzen JE, Boogers MJ, Kroft LJ, de Roos A, et al. Diagnostic Accuracy of 320-Row Multidetector Computed Tomography Coronary Angiography to Noninvasively Assess In-Stent Restenosis. Investigative Radiology. 2010 Jun;45(6):331. doi:10.1097/RLI.0b013e3181dfa312
4. Dai T, Wang J rong, Hu P fei. Diagnostic performance of computed tomography angiography in the detection of coronary artery in-stent restenosis: evidence from an updated meta-analysis. Eur Radiol. 2018 Apr;28(4):1373–82. doi:10.1007/s00330-017-5097-0
5. Yuan M, Wu H, Li R, Yu M, Dai X, Zhang J. The value of quantified plaque analysis by dual-source coronary CT angiography to detect vulnerable plaques: a comparison study with intravascular ultrasound. Quant Imaging Med Surg. 2020 Mar;10(3):668–77. doi:10.21037/qims.2020.01.13
6. Christine Quast M., Raphael Phinicarides M., Shazia Afzal M., et al. Roadmap Fusion Imaging in Percutaneous Coronary Intervention Reduces Contrast Medium Exposure Irrespective of Investigator's Experience Level. Journal of Invasive Cardiology 2024;36(1).
7. Azam MA, Khan KB, Salahuddin S, Rehman E, Khan SA, Khan MA, et al. A review on multimodal medical image fusion: Compendious analysis of medical modalities, multimodal databases, fusion techniques and quality metrics. Computers in Biology and Medicine. 2022 May;144:105253. doi:10.1016/j.compbiomed.2022.105253
8. Bertsche D, Rottbauer W, Rasche V, Buckert D, Markovic S, Metze P, et al. Computed tomography angiography/magnetic resonance imaging-based preprocedural planning and guidance in the interventional treatment of structural heart disease. Front Cardiovasc Med. 2022 Oct 17;9:931959. doi:10.3389/fcvm.2022.931959
9. Wu PW, Tsay PK, Sun Z, Peng SJ, Lee CY, Hsu MY, et al. Added Value of Computed Tomography Virtual Intravascular Endoscopy in the Evaluation of Coronary Arteries with Stents or Plaques. Diagnostics. 2022 Feb 3;12(2):390. doi:10.3390/diagnostics12020390
10. Hong SJ, Kim BK, Shin DH, Nam CM, Kim JS, Ko YG, et al. Effect of Intravascular Ultrasound-Guided vs Angiography-Guided Everolimus-Eluting Stent Implantation: The IVUS-XPL Randomized Clinical Trial. Intravascular Ultrasound. 2015.
11. Shlofmitz E, Torguson R, Zhang C, Mintz GS, Dheendsa A, Khalid N, et al. Impact of intravascular ultrasound on Outcomes following PErcutaneous coronary interventioN for In-stent Restenosis (iOPEN-ISR study). International Journal of Cardiology. 2021 Oct;340:17–21. doi:10.1016/j.ijcard.2021.08.003
12. Garcìa-Garcìa HM, Gogas BD, Serruys PW, Bruining N. IVUS-based imaging modalities for tissue characterization: similarities and differences. Int J Cardiovasc Imaging. 2011 Feb;27(2):215–24. doi:10.1007/s10554-010-9789-7
13. Räber L, Mintz GS, Koskinas KC, Johnson TW, Holm NR, Onuma Y, et al. Clinical use of intracoronary imaging. Part 1: guidance and optimization of coronary interventions. An expert consensus document of the European Association of Percutaneous Cardiovascular Interventions. European Heart Journal. 2018 Sep 14;39(35):3281–300. doi:10.1093/eurheartj/ehy285
14. Lenz T, Nicol P, Castellanos MI, Abdelgalil AAA, Hoppmann P, Kempf W, et al. Are we curing one evil with another? A translational approach targeting the role of neoatherosclerosis in late stent failure. European Heart Journal Supplements. 2020 Apr 1;22(Supplement_C):C15–25. doi:10.1093/eurheartj/suaa006
15. Calvert PA, Obaid DR, O'Sullivan M, Shapiro LM, McNab D, Densem CG, et al. Association Between IVUS Findings and Adverse Outcomes in Patients with Coronary Artery Disease. JACC: Cardiovascular Imaging. 2011 Aug;4(8):894–901. doi:10.1016/j.jcmg.2011.05.005
16. Yamada R, Okura H, Kume T, Neishi Y, Kawamoto T, Miyamoto Y, et al. A comparison between 40 MHz intravascular ultrasound iMap imaging system and integrated backscatter intravascular ultrasound. Journal of Cardiology. 2013 Feb;61(2):149–54. doi:10.1016/j.jjcc.2012.10.008
17. Tanita A, Sunamura S, Ogata T, Noda K, Takii T, Nitta Y, et al. Correlation between coronary angioscopy yellow grade and lipid plaque assessment by integrated backscatter intravascular ultrasound. Cardiovasc Interv and Ther. 2025 May 27. doi:10.1007/s12928-025-01133-6
18. Kawasaki M, Takatsu H, Noda T, Sano K, Ito Y, Hayakawa K, et al. *In Vivo* Quantitative Tissue Characterization of Human Coronary Arterial Plaques by Use of Integrated Backscatter Intravascular Ultrasound and Comparison with Angioscopic Findings. Circulation. 2002 May 28;105(21):2487–92. doi:10.1161/01.CIR.0000017200.47342.10
19. Joner M, Koppara T, Byrne RA, Castellanos MI, Lewerich J, Novotny J, et al. Neoatherosclerosis in Patients with Coronary Stent Thrombosis: Findings From Optical Coherence Tomography Imaging (A Report of the PRESTIGE Consortium). JACC: Cardiovascular Interventions. 2018 Jul;11(14):1340–50. doi:10.1016/j.jcin.2018.02.029
20. Erdogan E, Bajaj R, Lansky A, Mathur A, Baumbach A, Bourantas CV. Intravascular Imaging for Guiding In-Stent Restenosis and Stent Thrombosis Therapy. JAHA. 2022 Nov 15;11(22):e026492. doi:10.1161/JAHA.122.026492
21. Ñato M, Gomez-Lara J, Romaguera R, Roura G, Ferreiro JL, Teruel L, et al. One-year optical coherence tomography findings in patients with late and very-late stent thrombosis treated with intravascular imaging guided percutaneous coronary intervention. Int J Cardiovasc Imaging. 2018 Oct;34(10):1511–20. doi:10.1007/s10554-018-1372-7
22. Bergmark BA, Golomb M, Kuder JF, Buccola J, Wollmuth J, Lopez J, et al. ISR vs *De Novo* Lesion Treatment During OCT-Guided PCI: Insights from the LightLab Initiative. Journal of the Society for Cardiovascular Angiography & Interventions. 2023 Nov;2(6):101118. doi:10.1016/j.jscai.2023.101118
23. Koskinas KC, Nakamura M, Räber L, Colleran R, Kadota K, Capodanno D, et al. Current use of intracoronary imaging in interventional practice – Results of a European Association of Percutaneous Cardiovascular Interventions (EAPCI) and Japanese Association of Cardiovascular Interventions and Therapeutics (CVIT) Clinical Practice Survey. Doi: 10.4244/EIJY18M03_01.
24. Leistner DM, Riedel M, Steinbeck L, Stähli BE, Fröhlich GM, Lauten A, et al. Real-time optical coherence tomography coregistration with angiography in percutaneous coronary intervention–impact on physician decision-making: The OPTICO-integration study. Catheterization and Cardiovascular Interventions. 2018;92(1):30–7. doi:10.1002/ccd.27313
25. IJsselmuiden AJJ, Zwaan EM, Oemrawsingh RM, Bom MJ, Dankers FJWM, De Boer MJ, et al. Appropriate use criteria for optical coherence tomography guidance in percutaneous coronary interventions: Recommendations of the

working group of interventional cardiology of the Netherlands Society of Cardiology. Neth Heart J. 2018 Oct;26(10):473–83. doi:10.1007/s12471-018-1143-z
26. Lacaita PG, Luger A, Troger F, Widmann G, Feuchtner GM. Photon-Counting Detector Computed Tomography (PCD-CT): A New Era for Cardiovascular Imaging? Current Status and Future Outlooks. JCDD. 2024 Apr 21;11(4):127. doi:10.3390/jcdd11040127
27. Pijls NH, Van Son JA, Kirkeeide RL, De Bruyne B, Gould KL. Experimental basis of determining maximum coronary, myocardial, and collateral blood flow by pressure measurements for assessing functional stenosis severity before and after percutaneous transluminal coronary angioplasty. Circulation. 1993 Apr;87(4):1354–67. doi:10.1161/01.CIR.87.4.1354
28. Kwon W, Choi KH, Lee SH, Hong D, Shin D, Kim HK, et al. Clinical Value of Single-Projection Angiography–Derived FFR in Noninfarct-Related Artery. Circ: Cardiovascular Interventions. 2024 May;17(5). doi:10.1161/CIRCINTERVENTIONS.123.013844
29. Tsigkas GG, Bourantas GC, Moulias A, Karamasis GV, Bekiris FV, Davlouros P, et al. Rapid and Precise Computation of Fractional Flow Reserve from Routine Two-Dimensional Coronary Angiograms Based on Fluid Mechanics: The Pilot FFR2D Study. JCM. 2024 Jun 29;13(13):3831. doi:10.3390/jcm13133831
30. Faes TJC, Meer R, Heyndrickx GR, Kerkhof PLM. Fractional Flow Reserve Evaluated as Metric of Coronary Stenosis—A Mathematical Model Study. Front Cardiovasc Med. 2020 Jan 14;6:189. doi:10.3389/fcvm.2019.00189
31. Piroth Z, Otsuki H, Zimmermann FM, Ferenci T, Keulards DCJ, Yeung AC, et al. Prognostic Value of Measuring Fractional Flow Reserve After Percutaneous Coronary Intervention in Patients with Complex Coronary Artery Disease: Insights from the FAME 3 Trial. Circ: Cardiovascular Interventions. 2022 Nov;15(11):884–91. doi:10.1161/CIRCINTERVENTIONS.122.012542
32. Hidalgo F, González-Manzanares R, Ojeda S, Pastor-Wulf D, Flores G, Gallo I, et al. Jailed pressure wire technique for coronary bifurcation lesions: structural damage and clinical outcomes. Revista Española de Cardiología (English Edition). 2023 Jul;76(7):531–8. doi:10.1016/j.rec.2022.11.004
33. Sen S, Escaned J, Malik IS, Mikhail GW, Foale RA, Mila R, et al. Development and Validation of a New Adenosine-Independent Index of Stenosis Severity from Coronary Wave–Intensity Analysis. Journal of the American College of Cardiology. 2012 Apr;59(15):1392–402. doi:10.1016/j.jacc.2011.11.003
34. Seitz A, Baumann S, Sechtem U, Ong P. Optimal Prognostication of Patients with Coronary Stenoses in the Pre- and Post-PCI setting: Comments on TARGET FFR and DEFINE-FLOW Trials Presented at TCT Connect 2020. Eur Cardiol. 2021 Apr 27;16:e17. doi:10.15420/ecr.2021.04
35. Lee JM, Jung JH, Hwang D, Park J, Fan Y, Na SH, et al. Coronary Flow Reserve and Microcirculatory Resistance in Patients with Intermediate Coronary Stenosis. Journal of the American College of Cardiology. 2016 Mar;67(10):1158–69. doi:10.1016/j.jacc.2015.12.053
36. Biondi-Zoccai G, Versaci F, Iskandrian AE, Schillaci O, Nudi A, Frati G, et al. Umbrella review and multivariate meta-analysis of diagnostic test accuracy studies on hybrid non-invasive imaging for coronary artery disease. Journal of Nuclear Cardiology. 2020 Oct 1;27(5):1744–55. doi:10.1007/s12350-018-01487-w
37. Davies JE, Sen S, Dehbi HM, Al-Lamee R, Petraco R, Nijjer SS, et al. Use of the Instantaneous Wave-free Ratio or Fractional Flow Reserve in PCI. New England Journal of Medicine. 2017 May 11;376(19):1824–34. doi:10.1056/NEJMoa1700445
38. Berry C, Van 'T Veer M, Witt N, Kala P, Bocek O, Pyxaras SA, et al. VERIFY (VERification of Instantaneous Wave-Free Ratio and Fractional Flow Reserve for the Assessment of Coronary Artery Stenosis Severity in EverydaY Practice). Journal of the American College of Cardiology. 2013 Apr;61(13):1421–7. doi:10.1016/j.jacc.2012.09.065
39. Becker LM, Peper J, Van Nes SH, Van Es HW, Sjauw KD, Van De Hoef TP, et al. Non-invasive physiological assessment of coronary artery obstruction on coronary computed tomography angiography. Neth Heart J. 2024 Nov;32(11):397–404. doi:10.1007/s12471-024-01902-7
40. Michiels V, Andreini D, Conte E, Tanaka K, Belsack D, Nijs J, et al. Long term effects of surgical and transcatheter aortic valve replacement on FFRCT in patients with severe aortic valve stenosis [Internet]. 2022 Feb. doi:10.1007/s10554-021-02401-1
41. Hwang D, Koo BK, Zhang J, Park J, Yang S, Kim M, et al. Prognostic Implications of Fractional Flow Reserve After Coronary Stenting: A Systematic Review and Meta-analysis. JAMA Netw Open. 2022 Sep 22;5(9):e2232842. doi:10.1001/jamanetworkopen.2022.32842
42. Ried I, Krinke I, Adolf R, Krönke M, Moosavi SM, Hendrich E, et al. Incremental diagnostic value of coronary computed tomography angiography derived fractional flow reserve to detect ischemia. Sci Rep. 2025 Apr 14;15(1):12817. doi:10.1038/s41598-025-95597-4
43. Gonzalez JA, Lipinski MJ, Flors L, Shaw PW, Kramer CM, Salerno M. Meta-Analysis of Diagnostic Performance of Coronary Computed Tomography Angiography, Computed Tomography Perfusion, and Computed Tomography-Fractional Flow Reserve in Functional Myocardial Ischemia Assessment Versus Invasive Fractional Flow Reserve. The American Journal of Cardiology. 2015 Nov;116(9):1469–78. doi:10.1016/j.amjcard.2015.07.078
44. Yongguang G, Yibing S, Ping X, Jinyao Z, Yufei F, Yayong H, et al. Diagnostic efficacy of CCTA and CT-FFR based on risk factors for myocardial ischemia. J Cardiothorac Surg. 2022 Dec;17(1):39. doi:10.1186/s13019-022-01787-w
45. Lopezpalop R, Pinar E, Lozano I, Saura D, Pico F, Valdes M. Utility of the fractional flow reserve in the evaluation of angiographically moderate in-stent restenosis. European Heart Journal. 2004 Nov;25(22):2040–7. doi:10.1016/j.ehj.2004.07.016
46. Douglas PS, Nanna MG, Kelsey MD, Yow E, Mark DB, Patel MR, et al. Comparison of an Initial Risk-Based Testing Strategy vs Usual Testing in Stable Symptomatic Patients with Suspected Coronary Artery Disease: The PRECISE Randomized Clinical Trial. JAMA Cardiol. 2023 Oct 1;8(10):904. doi:10.1001/jamacardio.2023.2595
47. Hirai K, Kawasaki T, Sakakura K, Soejima T, Kajiyama K, Fukami Y, et al. Determinants of insufficient improvement in fractional flow reserve following percutaneous coronary intervention. Heart Vessels. 2020 Dec;35(12):1650–6. doi:10.1007/s00380-020-01645-6
48. Liu X, Xie Y, Diao S, Tan S, Liang X. Unsupervised CT Metal Artifact Reduction by Plugging Diffusion Priors in Dual Domains. IEEE Transactions on Medical Imaging. 2024 Oct;43(10):3533–45. doi:10.1109/TMI.2024.3351201
49. He W, Xu C, Wang X, Lei J, Qiu Q, Hu Y, et al. Development and validation of a risk prediction nomogram for in-stent restenosis in patients undergoing percutaneous coronary intervention. BMC Cardiovasc Disord. 2021 Dec;21(1):435. doi:10.1186/s12872-021-02255-4
50. Deng X, Deng Q, Zhang Q, Hou J. Association of systemic immune-inflammatory index with in-stent restenosis in patients with and without diabetes mellitus. Front Cardiovasc Med. 2025 Jan 20;12:1419314. doi:10.3389/fcvm.2025.1419314
51. Ohashi H, Takashima H, Ando H, Suzuki A, Sakurai S, Nakano Y, et al. Clinical feasibility of resting full-cycle ratio as a unique non-hyperemic index of invasive functional lesion assessment. Heart Vessels. 2020 Nov;35(11):1518–26. doi:10.1007/s00380-020-01638-5
52. Svanerud J, Ahn JM, Jeremias A, Van 'T Veer M, Gore A, Maehara A, et al. Validation of a novel non-hyperaemic index of coronary artery stenosis severity: the Resting Full-cycle Ratio (VALIDATE RFR) study. EuroIntervention. 2018 Sep;14(7):806–14. doi:10.4244/EIJ-D-18-00342
53. Muroya T, Kawano H, Hata S, Shinboku H, Sonoda K, Kusumoto S, et al. Relationship between resting full-cycle ratio and fractional flow reserve in assessments of coronary stenosis severity. Cathet Cardio Intervent. 2020 Oct;96(4). doi:10.1002/ccd.28835
54. Chuang MJ, Chang CC, Lee YH, Lu YW, Tsai YL, Chou RH, et al. Clinical assessment of resting full-cycle ratio and fractional flow reserve for coronary artery disease in a real-world cohort. Front Cardiovasc Med. 2022 Oct 25;9:988820. doi:10.3389/fcvm.2022.988820
55. Liou K, Ooi SY. Resting Full-Cycle Ratio (RFR) in the Assessment of Left Main Coronary Disease: Caution Required. Heart, Lung and Circulation. 2020 Aug;29(8):1256–9. doi:10.1016/j.hlc.2019.12.014
56. 2024 ESC Guidelines for the management of chronic coronary syndromes.
57. Mehta OH, Hay M, Lim RY, Ihdayhid AR, Michail M, Michael J, et al. Comparison of diagnostic performance between quantitative flow ratio, non-hyperemic pressure indices and fractional flow reserve. Cardiovascular Diagnosis and Therapy. 2020;10(3).
58. Westra J, Sejr-Hansen M, Koltowski L, Mejía-Rentería H, Tu S, Kochman J, et al. Reproducibility of quantitative flow ratio: the QREP study. EuroIntervention. 2022 Feb;17(15):1252–9. doi:10.4244/EIJ-D-21-00425
59. Xu B, Tu S, Song L, Jin Z, Yu B, Fu G, et al. Angiographic quantitative flow ratio-guided coronary intervention (FAVOR III China): a multicentre, randomised, sham-controlled trial. The Lancet. 2021 Dec;398(10317):2149–59. doi:10.1016/S0140-6736(21)02248-0
60. Andersen BK, Sejr-Hansen M, Maillard L, Campo G, Råmunddal T, Stähli BE, et al. Quantitative flow ratio versus fractional flow reserve for coronary revascularisation guidance (FAVOR III Europe): a multicentre, randomised, non-inferiority trial. The Lancet. 2024 Nov;404(10465):1835–46. doi:10.1016/S0140-6736(24)02175-5
61. Gutiérrez-Chico JL, Chen Y, Yu W, Ding D, Huang J, Huang P, et al. Diagnostic accuracy and reproducibility of optical flow ratio for functional evaluation of coronary stenosis in a prospective series. Cardiol J. 2020 Sep 10;27(4):350–61. doi:10.5603/CJ.a2020.0071
62. Hong H, Jia H, Zeng M, Gutiérrez-Chico JL, Wang Y, Zeng X, et al. Risk Stratification in Acute Coronary Syndrome by Comprehensive Morphofunctional Assessment With Optical Coherence Tomography. JACC: Asia. 2022 Aug;2(4):460–72. doi:10.1016/j.jacasi.2022.03.004
63. Chen H, Li B, Xiao Y, Wang H, Kuang M, Sun H, et al. Diagnostic efficacy of the optical flow ratio in patients with coronary heart disease: A meta-analysis. Widmer RJ, editor. PLoS ONE. 2023 May 10;18(5):e0285508. doi:10.1371/journal.pone.0285508
64. Baumbach A, Bourantas CV, Serruys PW, Wijns W. The year in cardiology: coronary interventions The year in cardiology 2019. Cardiologia Croatica. 2020 Apr;15(5–6):114–31. doi:10.15836/ccar2020.114
65. Yu W, Tanigaki T, Ding D, Wu P, Du H, Ling L, et al. Accuracy of Intravascular Ultrasound-Based Fractional Flow Reserve in Identifying Hemodynamic Significance of Coronary Stenosis. Circ: Cardiovascular Interventions. 2021 Feb;14(2):e009840. doi:10.1161/CIRCINTERVENTIONS.120.009840
66. Sui Y, Yang M, Xu Y, Wu N, Qian J. Diagnostic performance of intravascular ultrasound-based fractional flow reserve versus angiography-based quantitative flow ratio measurements for evaluating left main coronary artery stenosis. Catheterization and Cardiovascular Interventions. 2022 Feb 7;99:1403–9. doi:10.1002/ccd.30078

67. Kubo T, Terada K, Ino Y, Shiono Y, Tu S, Tsao TP, et al. Combined Use of Multiple Intravascular Imaging Techniques in Acute Coronary Syndrome. Front Cardiovasc Med. 2022 Jan 17;8:824128. doi:10.3389/fcvm.2021.824128
68. Voros S, Rinehart S, Qian Z, Vazquez G, Anderson H, Murrieta L, et al. Prospective Validation of Standardized, 3-Dimensional, Quantitative Coronary Computed Tomographic Plaque Measurements Using Radiofrequency Backscatter Intravascular Ultrasound as Reference Standard in Intermediate Coronary Arterial Lesions. JACC: Cardiovascular Interventions. 2011 Feb;4(2):198–208. doi:10.1016/j.jcin.2010.10.008
69. Athanasiou L, Rigas G, Sakellarios AI, Exarchos TP, Siogkas PK, Bourantas CV, et al. Three-dimensional reconstruction of coronary arteries and plaque morphology using CT angiography – comparison and registration with IVUS. BMC Med Imaging. 2016 Dec;16(1):9. doi:10.1186/s12880-016-0111-6
70. Cao JJ, Shen L, Nguyen J, Rapelje K, Porter C, Shlofmitz E, et al. Accuracy and limitation of plaque detection by coronary CTA: a section-to-section comparison with optical coherence tomography. Sci Rep. 2023 Jul 22;13(1):11845. doi:10.1038/s41598-023-38675-9
71. Lee JM, Choi KH, Song YB, Lee JY, Lee SJ, Lee SY, et al. Intravascular Imaging–Guided or Angiography-Guided Complex PCI. N Engl J Med. 2023 May 4;388(18):1668–79. doi:10.1056/NEJMoa2216607
72. Jia H, Zhao C, Yu H, Wang Z, Liu H, Xu M, et al. Clinical performance of a novel hybrid IVUS-OCT system: a multicentre, randomised, non-inferiority trial (PANOVISION). EuroIntervention. 2023 Jul;19(4):e318–20. doi:10.4244/EIJ-D-22-01058
73. Kitahara S, Kataoka Y, Sugane H, Otsuka F, Asaumi Y, Noguchi T, et al. *In vivo* imaging of vulnerable plaque with intravascular modalities: its advantages and limitations. Cardiovasc Diagn Ther. 2020 Oct;10(5):1461–79. doi:10.21037/cdt-20-238
74. Szük T, et al. Impact of C-reactive protein on in-stent restenosis: a meta-analysis. Platelets. 2016 Jul 3;27(5):410–9. doi:10.3109/09537104.2015.1112368
75. Baktashian M, Saffar Soflaei S, Kosari N, Salehi M, Khosravi A, Ahmadinejad M, et al. Association of high level of hs-CRP with in-stent restenosis: A case-control study. Cardiovascular Revascularization Medicine. 2019 Jul;20(7):583–7. doi:10.1016/j.carrev.2018.08.015
76. Fu Y, Wu Y, Liu E. C-reactive protein and cardiovascular disease: From animal studies to the clinic (Review). Exp Ther Med. 2020 Jun 4;20(2):1211–9. doi:10.3892/etm.2020.8840
77. Clare J, Ganly J, Bursill CA, Sumer H, Kingshott P, De Haan JB. The Mechanisms of Restenosis and Relevance to Next Generation Stent Design. Biomolecules. 2022 Mar 10;12(3):430. doi:10.3390/biom12030430
78. Siahaan PP, Widiarti W, Saputra PBT, Putra RM, D'Oria M. Neutrophil-to-lymphocyte ratio as a potential biomarker in predicting in-stent restenosis: A systematic review and meta-analysis. Paramasivam G, editor. PLoS One. 2025 May 16;20(5):e0322461. doi:10.1371/journal.pone.0322461
79. Komura N, Tsujita K, Yamanaga K, Sakamoto K, Kaikita K, Hokimoto S, et al. Impaired Peripheral Endothelial Function Assessed by Digital Reactive Hyperemia Peripheral Arterial Tonometry and Risk of In-Stent Restenosis. JAHA. 2016 Jun 13;5(6):e003202. doi:10.1161/JAHA.116.003202
80. Zhang G, Yu H, Su J, Chi C, Su L, Wang F, et al. Identification of Key Genes Associated with Endothelial Cell Dysfunction in Atherosclerosis Using Multiple Bioinformatics Tools. Gladysheva I, editor. BioMed Research International. 2022 Jan;2022(1):5544276. doi:10.1155/2022/5544276
81. Aherrahrou R, Reinberger T, Hashmi S, Erdmann J. GWAS breakthroughs: mapping the journey from one locus to 393 significant coronary artery disease associations. Cardiovascular Research. 2024 Nov 5;120(13):1508–30. doi:10.1093/cvr/cvae161
82. Liu YW, Huang MS, Hsu LW, Chang HY, Lee CH, Lee CY, et al. Genetic risk model for in-stent restenosis of second-and third-generation drug-eluting stents. iScience. 2021 Sep;24(9):103082. doi:10.1016/j.isci.2021.103082
83. Sandstedt M, Marsh J, Rajendran K, Gong H, Tao S, Persson A, et al. Improved coronary calcification quantification using photon-counting-detector CT: an ex vivo study in cadaveric specimens. Eur Radiol. 2021 Sep;31(9):6621–30. doi:10.1007/s00330-021-07780-6
84. Sharma SP, Lemmens MJDK, Smulders MW, Budde RPJ, Hirsch A, Mihl C. Photon-counting detector computed tomography in cardiac imaging. Neth Heart J. 2024 Nov;32(11):405–16. doi:10.1007/s12471-024-01904-5
85. Emrich T, Hell M. Plaque composition on ultra-high-resolution coronary computed tomography angiography with optical coherence tomography correlation. European Heart Journal. 2023 May 14;44(19):1765–1765. doi:10.1093/eurheartj/ehac560
86. Meloni A, Maffei E, Clemente A, De Gori C, Occhipinti M, Positano V, et al. Spectral Photon-Counting Computed Tomography: Technical Principles and Applications in the Assessment of Cardiovascular Diseases. JCM. 2024 Apr 18;13(8):2359. doi:10.3390/jcm13082359
87. van der Bie J, Sharma SP, Hirsch A, Boccalini S, van Mieghem NM, Dijkshoorn ML, et al. Coronary Stent Imaging with Photon-counting Detector CT. Radiology: Cardiothoracic Imaging. 2025 Jun;7(3):e240338. doi:10.1148/ryct.240338
88. Hamasaki H, Arimura H, Yamasaki Y, Yamamoto T, Fukata M, Matoba T, et al. Noninvasive machine-learning models for the detection of lesion-specific ischemia in patients with stable angina with intermediate stenosis severity on coronary CT angiography. Phys Eng Sci Med. 2025 Mar;48(1):167–80. doi:10.1007/s13246-024-01503-z
89. Koetzier LR, Mastrodicasa D, Szczykutowicz TP. Deep Learning Image Reconstruction for CT: Technical Principles and Clinical Prospects.
90. Liang K, Zhang L, Yang H, Yang Y, Chen Z, Xing Y. Metal artifact reduction for practical dental computed tomography by improving interpolation-based reconstruction with deep learning. Medical Physics. 2019 Dec;46(12). doi:10.1002/mp.13644
91. Qayyum A, Qadir J, Bilal M, Al-Fuqaha A. Secure and Robust Machine Learning for Healthcare: A Survey. IEEE Reviews in Biomedical Engineering. 2021;14:156–80. doi:10.1109/RBME.2020.3013489